INTERNATIONAL JOURNAL OF MULTIDISCIPLINARY RESEARCH AND ANALYSIS

ISSN(print): 2643-9840, ISSN(online): 2643-9875

Volume 07 Issue 09 September 2024

DOI: 10.47191/ijmra/v7-i09-08, Impact Factor: 8.22

Page No. 4175-4180

Integrating the Hydrogenation of Nitrobenzene over Cu/Mgo Catalysts with the 1, 4-Butanediol Dehydrogenation Reaction

D. Subramanyam[1], Dr. N.P. Rathore[2]

[1]Research Scholar, Sri Satya Sai University of Technology & Medical Sciences, Sehore, Madhya Pradesh, India

[2]Professor, Department of Chemistry, Sri Satya Sai University of Technology & Medical Sciences, Sehore, Madhya Pradesh, India

ABSTRACT: Using a fixed bed reactor and Cu/MgO catalysts, the hydrogenation of nitrobenzene to aniline has been combined with the dehydrogenation of 1,4-butanediol to c-butyrolactone reaction in the vapour phase. These Cu/MgO catalysts were made using the co-precipitation method, and they were examined using techniques for BET surface area, XRD, TPR, and N2O pulse-chemisorption. It has been described how the hydrogenation of nitrobenzene over Cu/MgO catalysts coupled with the 1,4-butanediol dehydrogenation reaction has a positive effect**.**

KEYWORDS: Hydrogenation, Cu/MgO catalysts for 1,4-bu tanediol and c-butyrolactone dehydrogenation

1. INTRODUCTION

There are many benefits to coupling two opposing chemical transformations over a single catalyst bed, including operational simplicity [1], reduction of thermodynamic constraints [2], environmentally friendly operations [3], and improved product selectivities [4,5]. By combining the hydrogenation of furfural to 2-methylfuran with the dehydrogenation of cyclohexanol to cyclohexanone reaction over copper-based catalysts, Zheng et al. [1,5] recently demonstrated the advantages of reaction coupling. It has been demonstrated that a Cu-Zn catalyst works well for the coupling of the maleic anhydride hydrogenation and 1,4-butanediol dehydrogenation processes in terms of optimal hydrogen utilisation and improved energy efficiency [3]. Zhu et al. [4] reported similar benefits of reaction coupling by coupling the dehydrogenation of 1,4-butanediol reaction with the hydrogenation of maleic anhydride over Cu–Zn–Al catalyst.

In one of our most recent studies [6], we combined the hydrogenation of furfural to furfuryl alcohol with the dehydrogenation of cyclohexanol to cyclohexanone reaction over Cu-MgO-Cr2O3 catalyst in the vapour phase and discovered that the yields of the desired products, cyclohexanone and furfuryl alcohol, had been significantly increased. Here, we report for the first time the coupling of 1,4-butanediol dehydrogenation and nitrobenzene hydrogenation over Cu/MgO catalysts.

2. EXPERIMENTAL

2.1. Catalyst preparation:-

Co-precipitation was used to create Cu/MgO catalysts, and K2CO3 was used as a hydrolyzing agent. The necessary quantities of homogeneous aqueous salt solutions of Cu(NO3)2 3H2O and Mg(NO3)2 6H2O precursors were precipitated simultaneously at a pH of 9.0 under constant stirring at room temperature for the preparation of 15, 20, and 25 wt% Cu/MgO catalysts. Throughout the filtration process, the precipitated masses underwent several thorough washings with warm distilled water. The separated hydrated gels were dried at 393 K for 12 hours and then calcined at 723 K for 5 hours. The CM designation applies to these Cu/MgO catalysts. A 15 wt% Cu/MgO catalyst, for instance, is coded as 15CM..

2.2. Catalyst characterization

The potassium content of the diluted solution after the catalysts had been digested in aquaregia was determined by AAS (M/s. Perkin-Elmer A-300), which revealed that no appreciable amounts of K+ ion were present in the catalysts. A Miniplex X-ray diffractometer (M/s. Rigaku Corporation, Japan) with nickel-filtered Cu Ka radiation was used to record the X-ray diffraction

patterns for I calcined and (ii) reduced Cu/MgO catalysts.Using a SMART SORB 92/93 (M/s. SMART Instruments, India) under dynamic conditions, the N2 gas adsorption was carried out at 77 K.For the estimation of BET surface area, 30% N2/helium gas mixture, and for pore volume, 95% N2/helium gas mixtures were used.

On a DIY TPR system, temperature programmed reduction (TPR) studies of every catalyst were carried out [7]. At the centre of the quartz reactor, there was a concentration of about 50 mg of the catalyst sample (18/25 mesh sieved particles). From room temperature to 973 K, it is heated linearly in the reducing gas mixture (11% H2 in argon) at a rate of 5 K/min. An isothermal condition was then maintained for an additional 30 min. at 973 K.

The chemisorption of N2O was assessed using a homemade pulse reactor [7]. The catalyst sample was reduced at 553 K for 3 hours while flowing hydrogen, then cooled to 353 K while flowing helium (flushing). Pulses of a 10% N2O gas mixture (9.72% N2O and the remaining helium) were injected. The patterns were recorded using a common GC programme (Class GC 10). Cu/N2O stoichiometry of 2 was used to calculate the quantity of surface Cu metal atoms.

2.3. Catalytic activity

Atmospheric pressure catalytic experiments were conducted in a fixed bed reactor (10 mm i.d. and 200 mm long). Catalyst was loaded and reduced for three hours at 553 K in an H2 flow.

Beyond 553 K, the Cu component in catalysts is known to begin sintering. The reduction temperature is set at 553 K for this reason. In addition to N2 gas flowing at a rate of 17 ml/min, 1,4-butanediol and/or nitrobenzene were fed at a flow rate of 1 ml/h. H2 served as the reducing gas for the independent nitrobenzene reaction. H2:nitrobenzene feed composition was set at 4:1 with catalyst space velocity of 100 mmol/g. The products were gathered in a cold trap and periodically tested. The products were identified using the GCMS-QP-5050 (M/s. Shimadzu Instruments, Japan) and then examined using the GC, 17A (M/s. Shimadzu Instruments, Japan) and a ZBWAX capillary column.

3. RESULTS AND DISCUSSION

15CM, 20CM, and 25CM catalysts have BET surface areas of 20, 32, and 29 m^2/g, respectively. Compared to 15CM catalyst, the surface area of 20CM catalyst has significantly increased. The contribution of finely dispersed Cu species may explain the increase in surface area with increased Cu loading. The agglomeration of some of the finely dispersed Cu species may be the cause of the slight decrease in surface area that occurs when Cu loading is increased from 20% to 25%.

Fig. 1 shows the Cu/MgO catalysts' XRD patterns (calcined and reduced). Only a poorly crystalline phase of both CuO and MgO was visible in the XRD pattern of the 15CM calcined catalyst.The observed d values are well matched to the crystalline phase of CuO (d = 2.52_x (35.6^0), 2.32_x (38.78^0), and 2.535 (35.45^0); ASTM\sCard No.5-661). The crystalline phase of MgO was confirmed from the d values on the 2h scale (d = 2.11_x (42.82^0), 1.495 (62.25^0), and\s1.221 (78.30^0); ASTM card No. 4-829). Compared to the catalysts with 15% and 25% Cu loadings, the sizes of the CuO and MgO crystallites are smaller at 20% Cu loading. In fact, both CuO and MgO were nearly amorphous at 20% loading, possibly due to the formation of interacted species between CuO and MgO at this loading

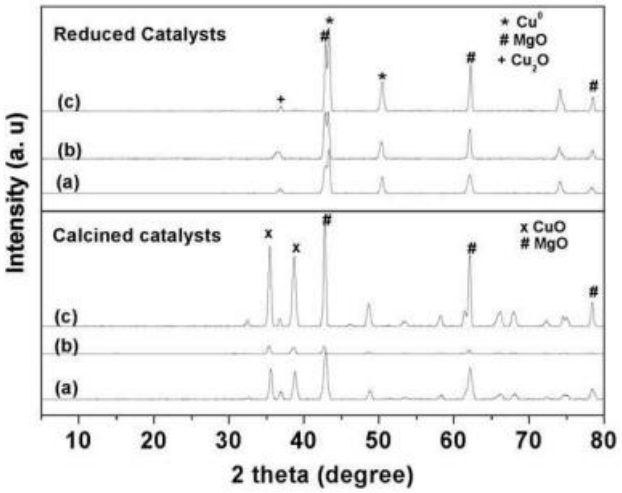

Fig. 1. XRD patterns of calcined and reduced Cu/MgO catalysts (a) 15CM, (b) 20CM, and (c) 25CM.

Table 1 includes the MgO and CuO crystallite sizes from XRD line broadening studies. It is evident from the XRD patterns of reduced

catalysts that the sizes of the Cu crystallites in all three loadings are essentially the same. This shows that during the reduction step, the phases of

Table 1
XRD and N_2O pulse chemisorption data of Cu/MgO catalysts.

Catalyst	XRD results						N_2O pulse chemisorption results			
	Crystallite size CuO/Cu (nm)		Crystallite size MgO (nm)		Intensity ratio		Dispersion (%)	Surface area (m^2/g)	Particle size (nm)	MSA (m^2/g)
	Calcined	Reduced	Calcined	Reduced	Calcined	Reduced				
15CM	77	60	57	94	1.23	1.20	11	33	91	1.5
20CM	61	64	76	105	0.88	1.07	18	59	55	2.5
25CM	90	68	110	180	0.89	0.93	7.4	30	128	1.3

Cu and MgO were redistributed. The following aspects of surface Cu species' surface sites, dispersion, metal surface area, and particle sizes can all be determined using N2O pulse chemisorption. Table 1 displays the N2O pulse chemisorption data for all of the Cu/MgO catalysts. With an increase in Cu loading from 15% to 20%, the quantity of surface Cu sites, Cu metal dispersion, and metal surface area all increase. Cu particle size, however, is significantly reduced. All of the aforementioned parameters show a reversal of trend as the Cu loading increases from 20% to 25%. The above parameters against Cu loading may be greatly influenced by metal support interaction. The higher dispersion of Cu species may be the cause of the 20CM's lower Cu particle sizes. The formation of larger particles in the 25CM catalyst may be caused by the aggregation of Cu species.

The sizes of the Cu crystallites in the reduced catalysts' XRD patterns and N2O pulse chemisorption data do not match. This is because there is a chance that some of the Cu may have oxidised since the reduced catalysts were exposed to air while being recorded for their XRD. The CuO that results from areal oxidation may be amorphous in nature. However, the in-situ reduction step was carried out before the N2O pulse chemisorption, which is why the crystallite sizes from these two techniques do not exactly match. It is appropriate to use N2O pulse chemisorption to measure the Cu crystallite sizes since that is what we are trying to do.

The MgO/CuO intensity ratio in calcined catalysts and the MgO/Cu intensity ratio in reduced catalysts have both been calculated because it is challenging to determine the precise intensities of MgO and CuO from XRD patterns. Also included in Table 1 was this data.It is evident from the MgO/CuO ratios that as the Cu loading increases, the ratio decreases up to 20% Cu loading and remains nearly constant after that loading. The MgO/Cu ratios show that there is a continuous decreasing trend with Cu loading, which is consistent with Cu loading.

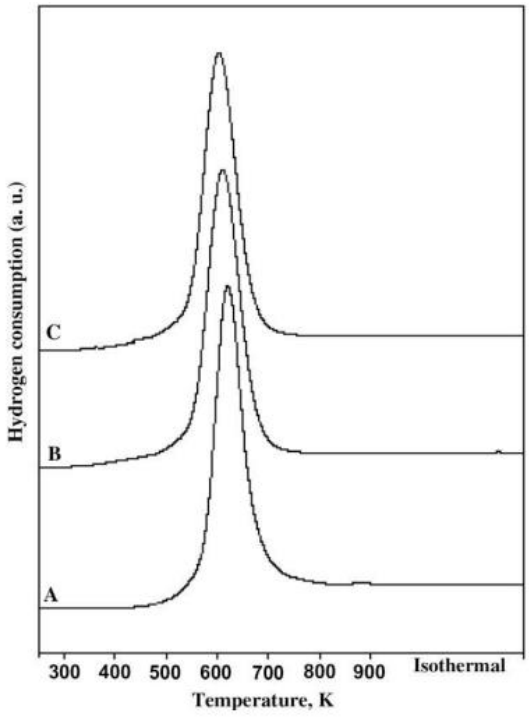

Fig. 2. TPR patterns of three Cu/MgO catalysts (A) 15CM, (B) 20CM, and (C) 25CM.

H2-TPR and the TPR profiles, which are shown in Fig. 2, were used to asses the reducibility of Cu/MgO catalysts. All three Cu/MgO catalysts displayed a single temperature maximum for reduction in the range of 610–630 K, which is consistent with the behaviour

of bulk CuO during reduction [8]. CuO is reduced starting at a temperature of about 500 K, and it continues up to a temperature of 750 K. Cu loading was increased from 15% to 25%, and as a result, the maximum reduction temperature decreased (15CM = 635 K, 20CM = 625 K, and 25CM = 610 K). Cu loading increases cause the reduction temperature to shift to the lower side, especially at higher Cu/Al2O3 catalyst loadings.The metal support interaction may be to blame for the higher reduction temperature at lower loadings. According to Chang et al. [10], the shift in this reduction temperature to lower values with an increase in Cu loading may be caused by the increased contribution of uniformly dispersed CuO crystallites. The TPR findings in this article were in good agreement with the reported single stage reduction literature [9]. In the higher loading catalysts, the majority of the Cu species reduce to the metallic state below 773 K [10].

In accordance with reaction Scheme 1, one mole of 1,4-butanediol results in two moles of hydrogen and one mole of c-butyrolactone.

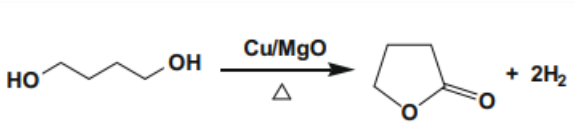

Scheme 1. Catalytic dehydrogenation of 1,4-butanediol to γ-butyrolactone.

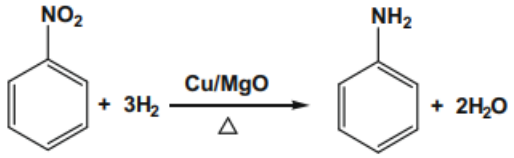

Scheme 2. Catalytic hydrogenation of nitrobenzene to aniline.

According to reaction scheme 2, one mole of nitrobenzene and three moles of hydrogen are needed to produce one mole of aniline. Hydrogen is produced in Scheme 1 while it is consumed in Scheme 2. Thus, without the need for external hydrogen pumping, these two reactions (Schemes 1 and 2) are coupled in the necessary mole ratios (Scheme 3).

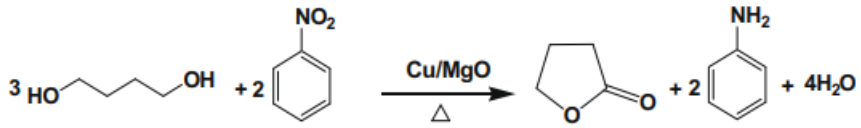

Scheme 3. Catalytic coupling of 1,4-butanediol dehydrogenation reaction with the hydrogenation of nitrobenzene.

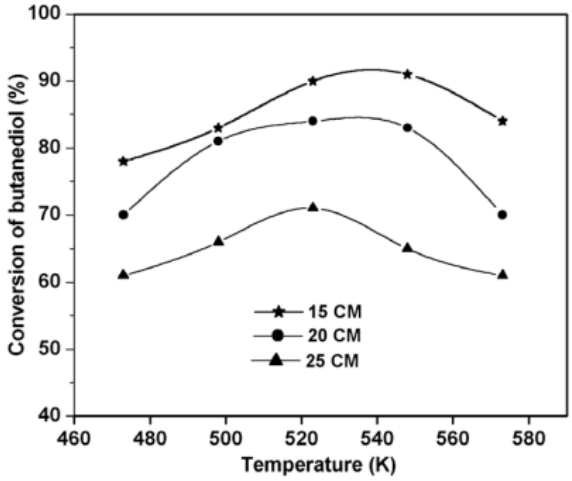

Fig. 3. Conversion of 1,4-butanediol versus reaction temperature over Cu/MgO catalysts.

Fig. 3 shows the 1,4-butanediol conversion with respect to reaction temperature over 15CM, 20CM, and 25CM catalysts. The conversion consistently improves as the reaction temperature rises from 473 to 523 K. Despite being an endothermic reaction, 1,4-butanediol dehydrogenation exhibits diminishing conversion at higher temperatures. From this study, it is unclear exactly why. It might, however, be the result of the sintering of copper particles or the deposition of coke. The performance of the three Cu/MgO catalysts is in the following order: 15CM > 20CM > 25CM. Of the three studied catalysts, 15CM catalyst demonstrated superior activity.

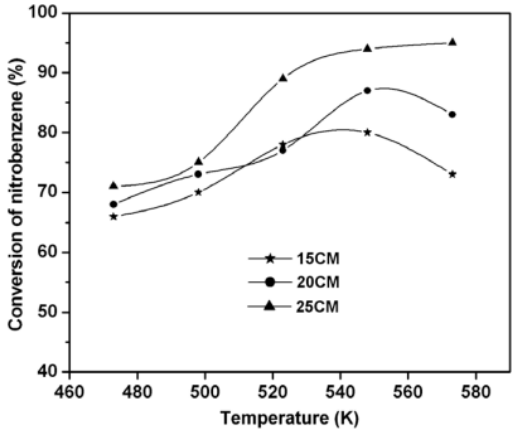

Fig. 4. Conversion of nitrobenzene versus reaction temperature over Cu/MgO catalysts.

Fig. 4 shows the outcomes of catalytic hydrogenation of nitrobenzene to aniline at various reaction temperatures using catalysts of 15CM, 20CM, and 25CM. The findings show that 25CM is the best-performing catalyst and that 553 K is the ideal reaction temperature. The catalytic activity is organized as follows: 25CM > 20CM > 15CM.

The reaction temperature is set at 523 K, and a 20CM catalyst has been chosen to couple the above two reactions based on the catalytic activity of the dehydrogenation of 1,4-butanediol and the hydrogenation of nitrobenzene over 15CM, 20CM, and 25CM catalysts.

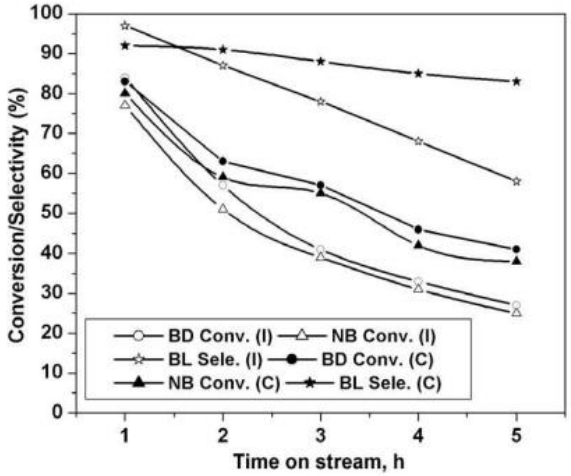

Fig. 5. Catalytic activity in the coupled reactions over 20CM catalysts at 523 K BD: 1,4-butanediol, NB: nitrobenzene, BL: c-butyrolactone(I): individual reaction, (C): coupled reaction.

Figure 5 displays the outcomes of 1,4-butanediol's catalytic dehydrogenation in the vapour phase and the hydrogenation of nitrobenzene with and without coupling over a 20CM catalyst. At the end of the fifth hour, the conversion of 1,4-butanediol and nitrobenzene in the independent reactions is significantly lower than that in the coupled reactions. The initial conversions for the two reactions, coupled and independent, are, however, nearly identical. At the end of the fifth hour, the selectivity of the independent reaction for c-butyrolactone is lower than it is for the coupled reaction for aniline, which is 100% throughout the duration of the stream.

It is not surprising that 1,4-butanediol conversion significantly increased and c-butyrolactone selectivity increased in the coupled reactions. The literature is replete with examples of how dehydrogenation activity increases when the right dehydrogenation reaction is combined with the right catalyst system [1–5]. According to the literature, Cyclohexanol dehydrogenation is thermodynamically constrained [1,6]. Due to the 1,4-butanediol dehydrogenation reaction's high equilibrium constant, K > 108 [3,4], no such thermodynamic restriction applies. Our earlier publications mentioned that activity is increased when the reverse water gas shift reaction is combined with the dehydrogenation of ethylbenzene [11–14]. When the hydrogenation of furfural to furfuryl alcohol is combined with the dehydrogenation of cyclohexanol to cyclohexanone, a higher conversion of cyclohexanol into cyclohexanone is observed [6]. The heat exchange between the exothermic hydrogenation and endothermic dehydrogenation

reactions can also be used to explain it.

The involvement of active hydrogen in the coupling reaction may be the cause of the improvement in the nitrobenzene conversion. Li and his colleagues have reported similar behaviour in the activity of hydrogenation reactions [3,4]. Dehydrogenation of ethylbenzene has been paired with hydrogenation of nitrobenzene, and it has been asserted that this combination significantly improved ethylbenzene conversion [15]. Catalyst deactivation is responsible for the rapid decline in conversion for independent reactions from 1 to 5 h. There will be a competitive adsorption between H2 and nitrobenzene in the independent reactions, especially in the nitrobenzene hydrogenation, where a significant amount of H2 is used in excess of nitrobenzene (H2/Nitrobenzene = 4). In the coupled reaction, nitrobenzene is immediately reacted with by H2 produced during the dehydrogenation of 1,4-butanediol before it desorbs from the catalyst surface. In other words, there will be competition between the two reactants to adsorb on catalyst surface because in the coupled reaction, H2 is in the adsorbed state, whereas in the independent reaction, nitrobenzene hydrogenation, H2 initially is in the gas phase. This could be the cause of the independent reactions' quick deactivation. Most likely, the hydrogen that is adsorbed to the catalyst's surface is essential in postponing the deactivation of the coupled reactions.

4. CONCLUSION

It can be said that the 1,4-butanediol and nitrobenzene independent reactions over Cu/MgO catalyst deactivate quickly. In contrast to independent reactions, the coupling reaction relies heavily on the presence of H2 in the adsorbed state to prevent the catalyst from deactivating to some extent.

REFERENCES

1) Gerardy, R., Debecker, D. P., Estager, J., Luis, P., & Monbaliu, J. C. M. (2020). Continuous flow upgrading of selected C2–C6 platform chemicals derived from biomass. *Chemical Reviews*, *120*(15), 7219-7347.
2) Rahimpour, M. R., Dehnavi, M. R., Allahgholipour, F., Iranshahi, D., & Jokar, S. M. (2012). Assessment and comparison of different catalytic coupling exothermic and endothermic reactions: A review. *Applied Energy*, *99*, 496-512.
3) Li, J., Shi, X. Y., Bi, Y. Y., Wei, J. F., & Chen, Z. G. (2011). Pd nanoparticles in ionic liquid brush: a highly active and reusable heterogeneous catalytic assembly for solvent-free or on-water hydrogenation of nitroarene under mild conditions. *ACS Catalysis*, *1*(6), 657-664.
4) Marella, R. K., Neeli, C. K. P., Kamaraju, S. R. R., & Burri, D. R. (2012). Highly active Cu/MgO catalysts for selective dehydrogenation of benzyl alcohol into benzaldehyde using neither O 2 nor H 2 acceptor. *Catalysis Science & Technology*, *2*(9), 1833-1838.
5) Su, M., Yang, R., & Li, M. (2013). Biodiesel production from hempseed oil using alkaline earth metal oxides supporting copper oxide as bi-functional catalysts for transesterification and selective hydrogenation. *Fuel*, *103*, 398-407.
6) B.M. Nagaraja, A.H. Padmasri, P. Seetharamulu, K. Hari Prasad Reddy, B. David Raju, K.S. Rama Rao, J. Mol. Catal. 278 (2007) 29.
7) B.M. Nagaraja, V. Siva Kumar, V. Shashikala, A.H. Padmasri, S. Sreevardhan Reddy, B. David Raju, K.S. Rama Rao, J. Mol. Catal. A 223 (2004) 339.
8) T. Nanba, S. Masukawa, J. Uchisawa, A. Obuchi, Catal. Lett. 93 (2004) 195.
9) T. Yamamoto, T. Tanaka, R. Kuma, S. Suzuki, F. Amano, Y. Shimooka, Y. Kohno, T. Funabiki, S. Yoshida, Phys. Chem. Phys. 4 (2002) 2449.
10) H.F. Chang, M.A. Slague, J. Mol. Catal. A: Chem. 88 (1994) 223.
11) B. David Raju, K.-M. Choi, J.-H. Lee, D.-S. Han, S.-E. Park, Catal. Commun. 8 (2007) 43.
12) B. David Raju, K.-M. Choi, D.-S. Han, Sujandi, N. Jiang, A. Burri, S.-E. Park, Catal. Today 131 (2008) 173.
13) B. David Raju, K.-M. Choi, D.-S. Han, J.-B. Koo, S.-E. Park, Catal. Today 115 (2006) 242.
14) B. David Raju, K.-M. Choi, S.-C. Han, A. Burri, S.-E. Park, J. Mol. Catal. 269 (2007) 58.
15) Z. Qin, J. Liu, A. Sun, J. Wang, Ind. Eng. Chem. Res. 42 (2003) 1329.